Electron-induced weak processes in ^{12}C and the behavior of the cross section near the maximal angle

S. L. Mintz
Physics Department, Florida International University, Miami, Florida 33199

M. Pourkaviani
Physics Department, University of Miami, Coral Gables, Florida 33124

(Received 6 January 1988)

Differential cross sections for the reaction $e^- + {}^{12}C \to \nu_e + {}^{12}B$ are obtained for the outgoing nucleus for incoming electron energies of 0.5, 1.5, 3.0, and 6.0 GeV near the maximal angle. A kinematic singularity at the maximal angle is investigated and eliminated by the use of a wave packet.

Recently[1] we have investigated the reaction $e^- + {}^{12}C \to \nu_e + {}^{12}B_{(g.s.)}$ and obtained differential cross sections in terms of the angle of outgoing nucleus. We found that a kinematical singularity occurred at the maximal angle leading to unbounded results. This singularity was not due to an infrared divergence and was associated only with the differential cross section for the final state nucleus, but not with the leptonic differential cross sections. In this Brief Report we study the singularity and show that it is a simple one which can be eliminated by using a wave packet for the final state nucleus and that the results for the differential cross section are essentially independent of the shape of the packet. We then obtain new differential cross sections for incident electron energies of 0.5, 1.5, 3.0, and 6.0 GeV.

From our previous results[1] we had obtained a differential cross section of the form

$$\frac{d\sigma}{d\Omega} = \frac{m_i G^2 \cos^2(\theta_c) p_f}{16\pi^2 E \mid m_i + E - [Ef \mid \mathbf{p}_e \mid \cos(\theta)/\mid \mathbf{p}_f \mid]\mid} \times \{ (F_M^2/8m_i^2 m_p^2)[Q^2(\nu\cdot e)^2 + (Q\cdot e)^2 \nu\cdot e + (Q\cdot\nu)^2\nu\cdot e] + F_A^2(e\cdot\nu + 2p_f\cdot\nu p_f\cdot e/m_f^2)$$
$$+ (F_M F_A/m_i m_p)\nu\cdot e(Q\cdot\nu + Q\cdot e) + (F_E F_A/2m_i m_p)[(\nu\cdot p_f - e\cdot p_f)/m_f^2](p_f\cdot e Q\cdot\nu + p_f\cdot\nu Q\cdot e - \nu\cdot e Q\cdot p_f)$$
$$+ (F_E^2 \mathbf{p}_f^2/16 m_i^2 m_p^2)(2Q\cdot e Q\cdot\nu - \nu\cdot e Q^2)\} , \quad (1)$$

where

$$M = [G\cos(\theta_c)/\sqrt{2}]\bar{u}_\nu \gamma^\mu (1-\gamma_5) u_e \langle {}^{12}B \mid J_\mu(0) \mid {}^{12}C \rangle , \quad (2)$$

and the vector and axial vector currents defined by $J_\mu(0) = V_\mu(0) - A_\mu(0)$ are given[2] by

$$\langle {}^{12}B \mid V_\mu(0) \mid {}^{12}C \rangle = -i\sqrt{2} m_i \epsilon_{\mu\delta\beta\gamma} q^\delta \xi^\beta Q^\gamma F_M(q^2)/(2m_i 2m_p) , \quad (3a)$$

$$\langle {}^{12}B \mid A_\mu(0) \mid {}^{12}C \rangle = \sqrt{2} m_i [\xi_\mu F_A(q^2) + q_\mu \xi\cdot q F_p(q^2)/m_\pi^2 - Q_\mu q\cdot\xi F_E(q^2)/(2m_i 2m_p)] , \quad (3b)$$

with $q_\mu = p_{f\mu} - p_{i\mu}$, $Q_\mu = p_{f\mu} + p_{i\mu}$, and $p_{f\mu}, p_{i\mu}$ being the ^{12}B and ^{12}C four momentum, respectively, m_f, m_i, and m_π being the ^{12}B, ^{12}C, and pion masses, respectively, and ξ_μ being the ^{12}B polarization vector.

We had also argued that the form factors $F_A(q^2)$, $F_M(q^2)$, and $F_E(q^2)$ could[3–5] be written as

$$F_i(q^2) = \frac{F_i(0)}{(1 - q^2/M_i^2)}, \quad i = A, M, E , \quad (4)$$

with $F_A(0) = 1.03$, $F_M(0) = 3.66$, and $F_E(0) = 3.75$ and $M_A^2 \approx M_M^2 \approx M_E^2 \approx 2.74 m_\pi^2$.

From conservation of energy and momentum, the energy of outgoing nucleus E_f in the laboratory frame may be written as

$$E_f = \frac{\rho\eta + \mid \mathbf{p}_e \mid \cos(\theta)[\eta^2 - 4m_f^2\rho^2 + 4\mathbf{p}_e^2 m_f^2 \cos^2(\theta)]^{1/2}}{2[\rho^2 - \mathbf{p}_e^2\cos(\theta)]} , \quad (5)$$

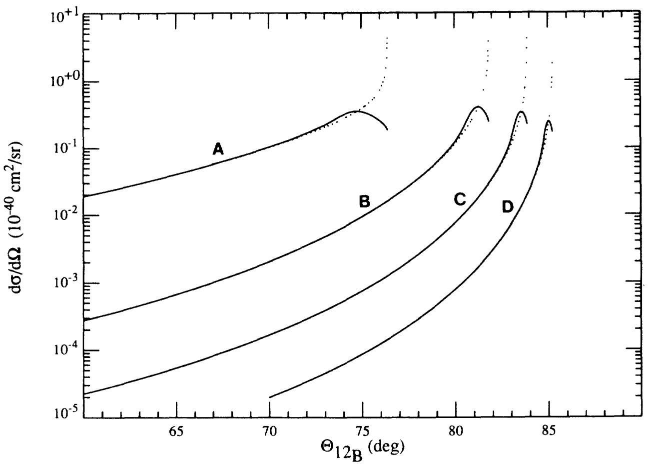

FIG. 1. Plot of the differential cross section for the process $e^- + {}^{12}C \rightarrow \nu_e + {}^{12}B$ as a function of outgoing ${}^{12}B$ laboratory angle. The solid curve is for a wave packet and the dotted curve is for a plane wave. Curves (A), (B), (C), and (D) are for $E = 0.5$, 1.5, 3.0, and 6.0 GeV, respectively.

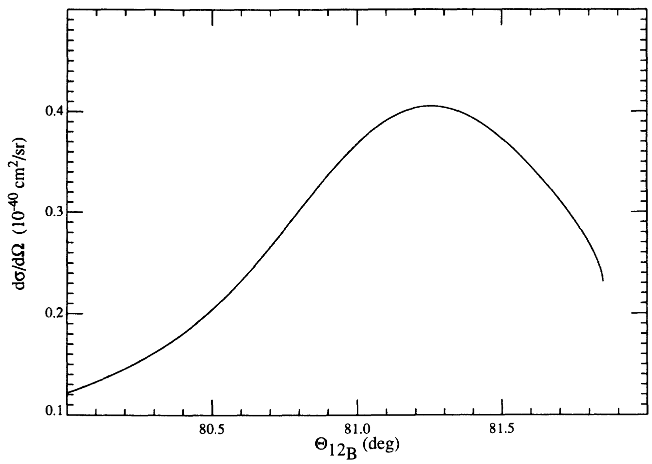

FIG. 3. Plot of the differential cross section for the process $e^- + {}^{12}C \rightarrow \nu_e + {}^{12}B$ as a function of outgoing ${}^{12}B$ laboratory angle for $E = 1.5$ GeV near the maximum angle for a wave packet.

where $\rho = m_i + E, \eta = \alpha + 2m_i E$, and $\alpha = m_i^2 + m_f^2 + m_e^2$. From this expression a maximal angle θ for the outgoing nucleus can be found and is given by

$$\sin(\theta) = 1 - \frac{\delta}{m_i} - \frac{\delta}{E} \tag{6}$$

to the lowest order in δ, $\delta \ll E$, m_i, where $\delta = m_f - m_i$.

Equation (6) is interesting because it shows that the maximal angle depends essentially on two terms. For large mass nuclei for which δ is small, the first term will not be very influential. However the δ / E term will be important for lower energy electrons and indeed, the maximal angle moves from about 76° for $E_e = 0.5$ GeV to about 85° for $E_e = 6.0$ GeV for the reaction being considered here.

As was previously noted,[1] the differential cross section $d\sigma / d\Omega_f$, Eq. (1), contains a singular term $1 / | m_i + E - [E_f \,|\mathbf{p}_e| \cos(\theta) / |\mathbf{p}_f| \,] |$ the denominator of which becomes zero at the maximal angle. We investigate the behavior of this term near the maximal angle, by writing $\theta = \theta_f - \epsilon$ where θ_f is the maximal angle and ϵ is an angle which we allow to become small. Then from Eq. (5), and a similar expression for $|\mathbf{p}_f|$, we obtain to the lowest order in ϵ,

$$| m_i + E - [E_f \,|\mathbf{p}_e| \cos(\theta) / |\mathbf{p}_f| \,] | \approx \frac{[\rho^2 - |\mathbf{p}_e^2| \cos^2(\theta_f)] 2m_f \sin^2(2\theta_f)}{\eta \cos(\theta_f)} \epsilon^{1/2} . \tag{7}$$

The important point here is that the singularity in $1 / | m_i + E - [E_f \,|\mathbf{p}_e| \cos(\theta) / |\mathbf{p}_f| \,] |$ is a very mild one, going as $\epsilon^{1/2}$. Thus if we more realistically assume a finite size for the outgoing nucleus, so that it is described

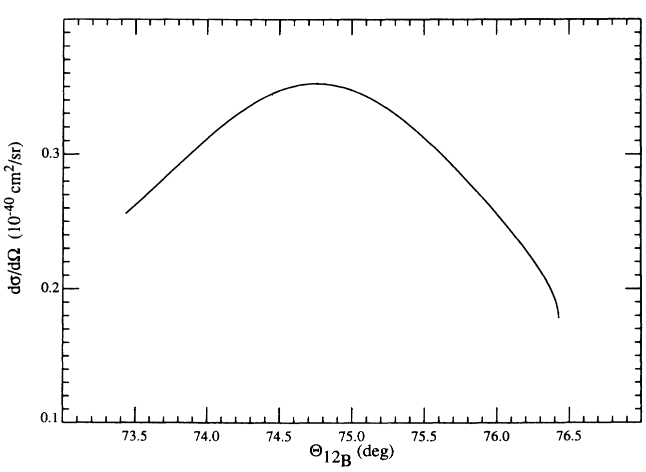

FIG. 2. Plot of the differential cross section for the process $e^- + {}^{12}C \rightarrow \nu_e + {}^{12}B$ as a function of outgoing ${}^{12}B$ laboratory angle for $E = 0.5$ GeV near the maximum angle for a wave packet.

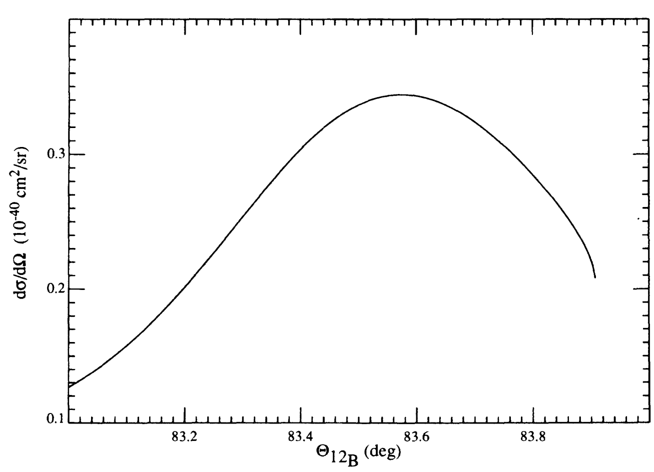

FIG. 4. Plot of the differential cross section for the process $e^- + {}^{12}C \rightarrow \nu_e + {}^{12}B$ as a function of outgoing ${}^{12}B$ laboratory angle for $E = 3.0$ GeV near the maximum angle for a wave packet.

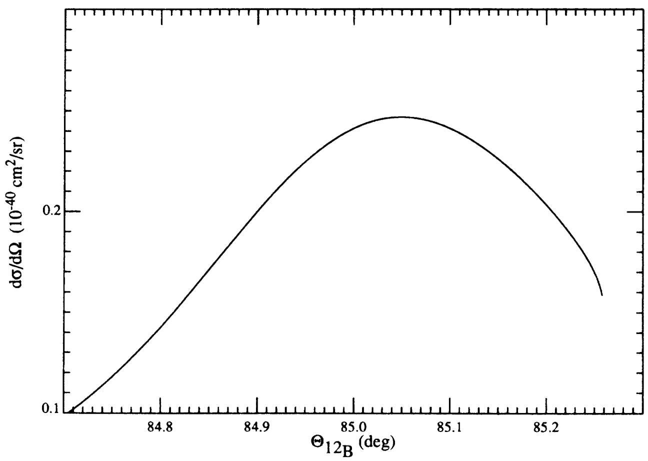

FIG. 5. Plot of the differential cross section for the process $e^- + {}^{12}C \to \nu_e + {}^{12}B$ as a function of outgoing ${}^{12}B$ laboratory angle for $E = 6.0$ GeV near the maximum angle for a wave packet.

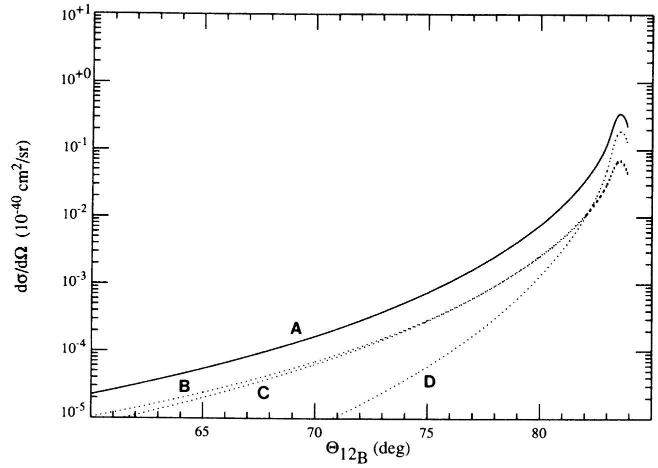

FIG. 6. Plot of the differential cross section for the process $e^- + {}^{12}C \to \nu_e + {}^{12}B$ as a function of outgoing ${}^{12}B$ laboratory angle for $E = 3.0$ GeV. Curve (A) is the total differential cross section. Curves (B), (C), and (D) are the contributions from F_M, F_E, and F_A, respectively.

by a packet, then this singularity will clearly be integrated away. We therefore look at $d\sigma/d\Omega_{\bar{f}}$ which is $d\sigma/d\Omega_f$ integrated over a packet

$$\frac{d\sigma}{d\Omega_{\bar{f}}} = \mathcal{N} \int f(x) e^{i(\mathbf{p}_{f_0} - \mathbf{p}_f)\cdot \mathbf{x}} \frac{d\sigma(p_f)}{d\Omega_f} d^3x \, d^3p_f \ , \tag{8}$$

so that

$$\frac{d\sigma}{d\Omega_{\bar{f}}} = \mathcal{N}' \int \chi(p_{f0}, p_f) \frac{d\sigma(p_f)}{d\Omega_f} d^3p_f \ , \tag{9}$$

where $\mathcal{N}$ and $\mathcal{N}'$ are the normalization factors.

We note that if our final state were described by a plane wave, χ would reduce to a delta function and $d\sigma/d\Omega_{\bar{f}} = d\sigma/d\Omega_f$ as expected. We note that we expect the packet $\chi(p_{f_0}, p_f)$ to be sharply peaked around p_{f0}. For convenience we use a Gaussian wave packet of *th* form

$$\chi(p_{f0}, p_f) = \frac{\alpha^3}{(2\pi)^{3/2}} e^{-\alpha^2(\mathbf{p} - \mathbf{p}_0)^2} \ . \tag{10}$$

However, we find that the shape does not play an important role in the result for $d\sigma/d\Omega_{\bar{f}}$. In fact because the singularity is in θ, we are able to perform all the other integration and treat the θ integration itself as an effective Gaussian of the form

$$\chi(\theta_f - \theta) = \frac{1}{\Delta(2\pi)^{1/2}} e^{-(\theta_f - \theta)^2/2\Delta^2} \ . \tag{11}$$

In Fig. 1, we show the results for $d\sigma/d\Omega_{\bar{f}}$ for $E = 0.5$, 1.5, 3.0, and 6.0 GeV where we have made use of Eq. (11) with

$$\Delta \approx \frac{(\Delta p)^2}{8\pi\sqrt{3} p_f^2 \sin(\theta_f)} \ . \tag{12}$$

We find substantial variations in Δ of Eq. (12), e.g., a factor of 2, are not sufficiently large to be visible in Fig. 1. We see that the effect of a proper treatment of the nucleus as a packet is to produce a definite maximum below the maximal angle and cause a fall off as maximal angle is approached. This is in line with the work[6] of Donnelly, Kronenberg, and Norum for a similar reaction on the ${}^3He \leftrightarrow {}^3H$ system. In Figs. 2, 3, 4, and 5 we show $d\sigma/d\Omega_{\bar{f}}$ near the maximal angle for the $E = 0.5$, 1.5, 3.0, and 6.0 GeV cases, respectively. We note that all of the differential cross sections peak in the 0.3 to 0.2×10^{-40} cm^2/sr range. Although these numbers are not very large, they are still several orders of magnitude larger than some already measured charged current reactions.[7]

Finally in the Fig. 6, we show the contributions from the individual form factors for $E = 3.0$ GeV. As can be seen the F_M and F_E contributions are comparable and larger than the F_A contribution for angles well below the maximal angle, but as the maximal angle is approached the contributions from the form factors would become comparable in size, i.e., 10^{-41} cm^2/sr, and by variations in E and θ one can get information about the size of these form factors. As defined $q^2 = m_i^2 + m_f^2 - 2m_i E_f$, and E_f is given by Eq. (5), so small variations in the incoming electron energy and outgoing nucleus angle can yield the same q^2 but different $d\sigma/d\Omega_{\bar{f}}$, hence it is possible in principle to determine F_M, F_E, and F_A simultaneously at a fixed value of q^2.

We note that although we have discussed only the ${}^{12}C \leftrightarrow {}^{12}B$ transition, the singularity is present for all nuclear transitions done by this method when the final state nucleus is examined. The resolution of the problem is exactly as given here for all cases.

Thus we see that if the formidable problems with background[1] can be overcome, electron induced weak processes in nuclei offer some hope for a systematic study of the weak hadronic current. Clearly much additional work including a careful study of background processes remains to be done.

[1]S. L. Mintz, Phys. Rev. C **36**, 860 (1987).
[2]S. L. Mintz, Phys. Rev. C **25**, 1671 (1982).
[3]F. Ajzenberg-Selove, Nucl. Phys. **A248**, 1 (1975).
[4]C. W. Kim and H. Primakoff, Phys. Rev. **140**, B566 (1965).
[5]W. Y. P. Hwang and H. Primakoff, Phys. Rev. C **16**, 397 (1977).
[6]T. W. Donnelly, E. L. Kronenberg, and B. E. Norum, *Research Program at CEBAF, Report of the 1985 Summer Study Group* (Newport News, Virginia, 1986) pp. 12–14.
[7]See, for example, T. L. Jenkins, F. E. Kinard, and F. Reines, Phys. Rev. **185**, 1599 (1969); and E. Pasierb *et al.*, Phys. Rev. Lett. **43**, 96 (1979).